

submitted to ApJ

Transit Timing Observations from *Kepler* : VI. Transit Timing Variation Candidates in the First Seventeen Months from Polynomial Models

Eric B. Ford¹, Darin Ragozzine², Jason F. Rowe^{3,4}, Jason H. Steffen⁵, Thomas Barclay^{3,6}, Natalie M. Batalha⁷, William J. Borucki³, Stephen T. Bryson³, Douglas A. Caldwell^{3,4}, Daniel C. Fabrycky^{8,9}, Thomas N. Gautier III¹⁰, Matthew J. Holman², Khadeejah A. Ibrahim¹¹, Hans Kjeldsen¹², Karen Kinemuchi^{3,6}, David G. Koch³, Jack J. Lissauer³, Martin Still^{3,6}, Peter Tenenbaum^{3,4}, Kamal Uddin¹¹, William Welsh¹³

eford@astro.ufl.edu

ABSTRACT

Transit timing variations provide a powerful tool for confirming and characterizing transiting planets, as well as detecting non-transiting planets. We report the results an updated TTV analysis for 822 planet candidates (Borucki

¹Astronomy Department, University of Florida, 211 Bryant Space Sciences Center, Gainesville, FL 32111, USA

²Harvard-Smithsonian Center for Astrophysics, 60 Garden Street, Cambridge, MA 02138, USA

³NASA Ames Research Center, Moffett Field, CA, 94035, USA

⁴SETI Institute, Mountain View, CA, 94043, USA

⁵Fermilab Center for Particle Astrophysics, P.O. Box 500, MS 127, Batavia, IL 60510

⁶Bay Area Environmental Research Institute, 560 Third St West, Sonoma, CA 95476, USA

⁷San Jose State University, San Jose, CA 95192, USA

⁸UCO/Lick Observatory, University of California, Santa Cruz, CA 95064, USA

⁹Hubble Fellow

¹⁰Jet Propulsion Laboratory/California Institute of Technology, Pasadena, CA 91109, USA

¹¹Orbital Sciences Corporation/NASA Ames Research Center, Moffett Field, CA 94035, USA

¹²Department of Physics and Astronomy, Aarhus University, DK-8000 Aarhus C, Denmark

¹³San Diego State University, 5500 Campanile Drive, San Diego, CA 92182-1221, USA

et al. 2011; Batalha et al. 2012) based on transit times measured during the first seventeen months of *Kepler* observations (Rowe et al. 2012). We present 35 TTV candidates (4.1% of suitable data sets) based on long-term trends and 153 mostly weaker TTV candidates (18% of suitable data sets) based on excess scatter of TTV measurements about a linear ephemeris. We anticipate that several of these planet candidates could be confirmed and perhaps characterized with more detailed TTV analyses using publicly available *Kepler* observations. For many others, *Kepler* has observed a long-term TTV trend, but an extended *Kepler* mission will be required to characterize the system via TTVs. We find that the occurrence rate of planet candidates that show TTVs is significantly increased ($\sim 60\%$ - 76%) for planet candidates transiting stars with multiple transiting planet candidate when compared to planet candidates transiting stars with a single transiting planet candidate.

Subject headings: planetary systems; planets and satellites: detection, dynamical evolution and stability; techniques: miscellaneous

1. Introduction

Long-term, high-precision photometric observations from NASA’s *Kepler* mission provide the basis for confirming and characterizing planets via transit timing variations (TTVs). *Kepler* has confirmed 10 transiting planets via TTVs (Holman et al. 2010; Ballard et al. 2011; Cochran et al. 2011; Lissauer et al. 2011a). Many more *Kepler* planet candidates are expected to reveal significant TTVs, as the time baseline of *Kepler* observations grows (Ford et al. 2011; hereafter F11). F11 reported preliminary indications of TTVs for dozens of additional planet candidates and predicted significant TTVs for several planet candidates in multiple transiting planet candidate systems based on the first fourth months of *Kepler* observations. This paper and Steffen et al. (2012b) provide updated TTV analyses of *Kepler* planet candidates to identify planets candidates worthy of more detailed TTV analyses. We describe our methods in §2. Table 1 provides a description of the online-only, machine-readable material in Table 2. We provide an overview of our results and discuss a subset of particularly interesting systems in §4.

2. Methods

We analyze transit times observed by *Kepler* through the end of quarter six (September 20, 2010) as reported in Rowe et al. (2012; hereafter R12). Following R12, we include planet candidates from Borucki et al. (2011a), as well as some more recent planet candidates for which planet properties will appear in Batalha et al. (2012). In particular, we include only planet candidates from Batalha et al. (2012) that transit stars for which there was already at least one planet candidates identified by Borucki et al. (2011). Regardless of whether the planet candidate was identified by Borucki et al. (2011) or Batalha et al. (2012), we analyze transit times only for planet candidates for which the photometric signal-to-noise of a typical transit is at least three.

For each planet candidate to be analyzed, we calculate the best-fit linear ephemeris (L_1) to the transit times and uncertainties from R12. We anticipate that the distribution of transit timing errors is likely to be approximated by a mixture distribution with heavily weighted Gaussian component (core) and a weakly weighted distribution with broader tails, due to the difficulties of measuring transit times (e.g., data artifacts, stellar variability, nearly simultaneous transit of another planet, large transit timing variations, or other complications). In order to reduce the effects of a small number of poorly measured transit times, we do not report the initial best-fit linear ephemeris (L_1), but rather report an updated linear ephemeris (L_2) calculated after cleaning the transit times to exclude outliers and transit times with unusually large uncertainties. Specifically, we reject any transit times with an absolute deviation from the linear ephemeris exceeding four times the median absolute deviation of transit times from the first linear ephemeris (L_1). We also reject any transit times for which the measurement uncertainty exceeds twice the median of the published transit time uncertainties. We record the median timing uncertainty for the remaining N_{TT} transit times (σ_{TT}). Then, we calculated an updated the best-fit linear ephemeris (L_2) using the cleaned transit times. We report the epoch (E_{lin}) and period (P_{lin}) of the updated linear ephemeris (L_2) in Table 2.

First, we identify planet candidates with larger than expected scatter about the updated linear ephemeris (L_2) in the measured transit times based on the measurement uncertainties (hereafter “excess scatter”). We calculate the median absolute deviation (MAD) and the weighted root mean square deviation (WRMS) of the clipped transit times relative to the updated linear ephemeris (F11). We calculate the p -value for a standard χ^2 test, $p_{\chi^2,lin}$ which is the porability that we would measure a χ^2 as large or larger than χ_{lin}^2 assuming transit timing errors follow a Gaussian distribution. We also calculate ($p_{\chi'^2,lin}$), the p -value for a χ^2 -test using $\chi'^2 = \pi N_{TT}(\text{MAD})^2/(2\sigma_{TT}^2)$, as described in F11. Since we cannot be confident that the transit time errors follow a Gaussian distribution, one should interpret the

listed p -values with caution (particularly for low S/N transits). We consider a small p -value as indicating that a transit timing data set is worthy of further investigation. We identify planet candidates with a $p_{\chi^2, \text{lin}} < 10^{-3}$ and/or $p_{\chi'^2, \text{lin}} < 10^{-3}$ by setting the 1 and 2 bits of the TTV flag (see Table 2). For a few planet candidates, the transit times have a small number of transits, but each has a highly significant deviation from a linear ephemeris. We indicate these ($\text{MAD} \geq 5\sigma_{TT}$) with the 3rd bit (with a value of 4) of the TTV flag.

Second, we identify planet candidates with long-term trends in the the deviations of the measured transit times from a linear ephemeris (hereafter referred to as “long-term TTV trends”). We calculate the best-fit (minimum χ^2) n_d -degree polynomial ephemeris

$$\hat{t}_n = E_{n_d} + n \times P_{n_d} \left(1 + \sum_{i=2}^{n_d} c_i n^{i-1} \right), \quad (1)$$

where \hat{t}_n is the predicted transit time of the n th transit, E_{n_d} and P_{n_d} are the epoch and period of the n_d -degree model and the c_i ’s are the higher-order coefficients. Note that we renumber the transits relative to R12, so the epoch falls near the middle of the observed transits, reducing covariance between the epoch and period. We calculate $\chi_{n_d}^2$ for each n_d up to 4, if there are at least 8 transits and otherwise for $n_d < n_{\text{TT}} - 2$. We perform standard F -tests using the ratio of χ^2 for the n_d -degree polynomial model and all lower-degree ephemerides. If $p_{F, \text{quad}, \text{lin}}$, the p -value for the F -test comparing the linear and quadratic models is less than 2%, then we conclude that the difference in χ_{quad}^2 and χ_{lin}^2 is greater than one would expect due to mere fluctuations at the 2% significance level. Therefore, we accept the quadratic model and set the 4th bit (with a value of 8) of the TTV Flag in Table 2. We repeat the procedure for the cubic and then the quartic models, accepting the higher degree models if the F -test p -value is less than 2% when comparing the higher degree model to both the linear model and the last accepted model. We list N_d , the degree of the highest-degree accepted model, along with p -values for the various tests in Table 2.

3. Results

We identified 35 TTV candidates with long-term trends using simple polynomial models (see Figures 1, 2 and 3)¹. Of these, we approximate the TTVs with a quadratic model for 12 planet candidates (KOIs 168.01, 308.01, 448.02, 473.01, 784.01, 806.02, 886.01, 904.02, 1081.01, 1573.01, 1581.01, 1599.01), a cubic model for 15 planet candidates (KOIs 227.01,

¹Similar figures for additional planet candidates will be available at <http://www.astro.ufl.edu/~eford/data/kepler/>.

250.01, 277.01, 392.01, 456.01, 524.01, 738.01, 854.01, 884.02, 918.01, 1102.02, 1145.01, 1199.01, 1270.02, 1366.02) and a quartic model for 8 planet candidates (KOIs 103.01, 137.01, 142.01, 248.01, 377.01, 377.02, 984.01, 1436.02). Three planet candidates have extremely significant TTVs, but polynomial models did not provide a significant improvement in fit, due to the limited number of transits (351.02 and 806.01) or a complex signal that was not well approximated by a ≤ 4 th degree polynomial (872.01). While we regard these as relatively strong TTV candidates, more detailed analyses will be necessary before the planets are confirmed, as one must ensure that the TTVs are dynamical in origin and that we are not observing eclipse timing variations in a triple star system (Carter et al. 2011; Slawson et al. 2011; Steffen et al. 2011) that has been diluted so the eclipse depth is consistent with a planet transit.

For an additional 150 planet candidates, the measured transit times appear to have a scatter greater than that expected based on the measurement uncertainties. While we regard these as weaker TTV candidates, we are optimistic that many may be closely-packed multiple planet systems for which TTVs could characterize the planet masses and orbital properties. For example, Table 2 identifies several confirmed planets as having excess TTV scatter but without a significant long-term trend (KOI 72.01=Kepler-10b, KOI137.02=Kepler-18d, 157.02=Kepler-11d, 157.03=Kepler-11e, 203.01=Kepler-17b). Thus, we recommend these planet candidates with excess TTV scatter for further analysis, as well as long-term monitoring by *Kepler* using the 1-minute cadence to improve the number, accuracy and precision of transit time measurements.

We note that more detailed analyses have detected TTVs for several planets that were not identified as having a long-term trend or excess scatter by our analysis (e.g., Kepler-11b, Kepler-18c, Kepler-19b). Thus, we anticipate that more detailed analyses (particularly those that use short-cadence observations or systems with multiple transiting planet candidates) may confirm and characterize additional planets via TTVs.

This analysis significantly improves on that of F11, primarily due to the increased number and time span of transit timing observations now available. Of those with an obvious TTV pattern (TTV Flag of 1 in F11 Table 1), six of seven are identified as significant in our updated analysis. The one exception (KOI 928.01) was not included in our analysis, as it is now a known triple star (Steffen et al. 2011b). All six have a statistically significant long-term trend. Of the seven candidates with $p_{F,\text{quad,lin}} \leq 0.02$ from F11 (Table 5), only two were identified as TTV candidates in our updated analysis. As noted in F11, the small number of transits and small time span of observations was a significant limitation.

4. Discussion

We compare the frequency of TTV candidates according to orbital period, transit S/N and whether the host star has multiple transiting planet candidates. For this purpose, we restrict our attention to planet candidates with at least 5 transits (after clipping points with unusually large uncertainties or absolute deviations, as described in §2), leaving 981 TTV data sets, including 545 (436) planet candidates associated with KOIs that have a single (multiple) transiting planet candidates. We find 179 (18%) TTV data sets with some indication of potential TTVs (TTV Flag ≥ 1), including 78 (14%) and 101 (23%) for stars with single and multiple transiting planet candidates, respectively. We find 35 (3.6%) TTV data sets with a long-term trend ($N_d \geq 2$), including 15 (2.8%) and 20 (4.6%) for stars with single and multiple transiting planet candidates. Based on Monte Carlo simulations, the probability of these two subsets of KOIs have the same occurrence rate of long term TTV trends (some indication of TTVs) is 2.7% ($< 10^{-4}$). Thus, these results suggest that planets in systems with multiple transiting planet candidates are significantly more likely to show TTVs than planets in stars with a single known transiting planet, in contrast to the results of a similar analysis performed using just the first four months of Kepler data in Ford et al. (2011). Such comparisons provide information about the frequency of non-transiting planets with similar orbital distances as the transiting planets and can help break the degeneracy between planet abundance and the distributions of mutual inclinations (Lissauer et al. 2011b, Tremaine & Dong 2011). For small, but non-zero mutual inclinations, the probability of multiple planets transiting is increased for closely-spaced systems that are also likely to yield large TTVs. The true frequency of TTVs is likely to rise for both samples with more detailed analyses and as the time span of *Kepler* observations increases. Further analysis will be required to understand how these results are affected by potential complications (e.g., some multiple planet systems might be overlooked due to TTVs interfering with their detection or transit time measurement).

We divide the TTV data sets into two equal-sized samples according to orbital period. This results in dividing the sample at 12.8d. We find no significant difference in the frequency of planet candidates with some indication of potential TTVs (TTV Flag ≥ 1), but a 83% greater frequency of long-term TTV trends among planet candidates with orbital period greater than 12.8d (i.e., 12 (22) long-term trends for the short (long) period sub-samples). Such a trend is not unexpected, since the TTV signal amplitude scales with the orbital period.

We divide the TTV data sets into two equal-sized samples according to photometric S/N of the transits. We find $\sim 15\%$ more planet candidates with some indication of potential TTVs (TTV Flag ≥ 1) among the low S/N sample, but no difference in the frequency of

long-term TTV trends according to photometric S/N. The increased frequency of planet candidates with excess TTV scatter could be due to either an increased frequency of TTVs for small planets or an increased frequency of poor transit time measurements for low S/N planet candidates.

We recommend that observers planning follow-up observations of *Kepler* planet candidates check whether there are indications of significant TTVs. While most KOIs show TTVs that are small compared to the transit duration, some systems (e.g., KOI 806) have TTVs so large that they can affect the scheduling of follow-up observations (e.g., Tingley et al. 2011; Fabrycky et al. 2012). Based on synthetic planet populations (Lissauer et al. 2011b), we anticipate that $\sim 15 - 26\%$ of planets could have TTVs as large as the transit duration. Of course, the higher-order ephemerides should not be trusted to predict future transit times accurately, as extrapolations are often unreliable.

On sufficiently long timescales, most TTV are likely better modeled with periodic functions. Indeed, Steffen et al. (2012) have performed a complementary analysis using a sinusoidal model. A periodic model is likely superior for TTV signals once they have been observed for multiple TTV cycles. We caution TTV signatures can be quite complex (e.g., Veras et al. 2011), so one can not presume that a sinusoidal model is necessarily a better model until the TTV signal has been observed for multiple cycles. Further, polynomial models require fewer model parameters and do not require searching over many possible TTV frequencies, making polynomial models more sensitive to low-amplitude, long-term TTV signals. Thus, polynomial and sinusoidal TTV models are both important and complementary tools to search for TTV candidates. We anticipate that the sinusoidal model is likely more appropriate for TTV candidates that require a $N_d \geq 4$ degree model.

The largest planetary TTV signatures are likely to arise in systems in or near mean motion resonances, but the associated timescales are typically multiple years (Agol et al. 2005; Holman & Murray 2005; Veras et al. 2011; Veras & Ford 2011). Over timescales short compared to the TTV timescale, polynomial models can often approximate the dominant TTV signal with a minimal number of model parameters. On the other hand, a periodic TTV model requires at least five model parameters (and a minimum of six transits to assess a model). Searching over many possible TTV frequencies requires performing many statistical tests, reducing the sensitivity to small amplitude signals when only a single TTV cycle has been observed. For planets with orbital periods approaching a year, it will be important to analyze TTV signals using as few transits as possible. Borcuki et al. (2011b) obtained early TTV constraints for a planet in the habitable zone using just 3 transit times. For tightly-packed systems with multiple transiting planets, a full TTV analysis may be possible even with only ~ 6 transits per planet (e.g., Holman et al. 2010; Fabrycky et al. 2012). Thus,

we anticipate that polynomial TTV models will remain an important tool for assessing TTV candidates, particularly for planet candidates with long orbital periods, such as those approaching the habitable zone of solar-type stars.

We anticipate that many of the planet candidates with long-term TTV trends (see Fig. 1, 2 & 3) are likely to be confirmed with additional analysis. Such large and coherent trends are unlikely to be due to astrophysical noise or non-Gaussian measurement errors. In some cases, further observations and/or TTV analysis may lead to the detection of additional non-transiting planets (e.g., Ballard et al. 2011), or even small planets with large TTVs that were not detected by the standard *Kepler* planet search pipeline. In other cases, long-term TTV trends may be due to perturbations from stellar or brown dwarf companions rather than additional planets. It is also possible that a transiting planet candidate with TTVs is actually an eclipsing binary that is significantly diluted, so the transit depth is consistent with planetary transit, and a member of a triple star system (e.g., KOI 928.01; Steffen et al. 2011). It is less clear what fraction of the planet candidates with excess TTV scatter have dynamically induced TTVs, as opposed to an apparent TTV signal due to astrophysical noise (e.g., Désert et al. 2011) or non-Gaussian measurement errors. Nevertheless, we recommend that these candidates be subjected to more detailed TTV analysis, as some of these are planets in closely-packed systems with complex TTVs (e.g., Kepler-11; Lissauer et al. 2011a). Such systems are particularly favorable for measuring planet masses and bulk density, so as to constrain the planet’s composition and nature (i.e., distinguish between rocky versus gaseous planets).

Funding for this mission is provided by NASA’s Science Mission Directorate. We thank the entire *Kepler* team for the many years of work that is proving so successful. E.B.F acknowledges support by the National Aeronautics and Space Administration under grant NNX08AR04G issued through the *Kepler* Participating Scientist Program. *Facilities:* *Kepler*.

REFERENCES

- Agol, E., Steffen, J., Sari, R., & Clarkson, W. 2005, MNRAS, 359, 567
- Ballard, S., Fabrycky, D., Fressin, F., et al. 2011, ApJ, 743, 200
- Batalha, N. M., et al. 2012, to be submitted to ApJS.
- Borucki, W. J., Koch, D. G., Basri, G., et al. 2011a, ApJ, 736, 19

- Borucki, W. J., Koch, D. G., Batalha, N., et al. 2011b, accepted to ApJ, arXiv:1112.1640
- Carter, J. A., Fabrycky, D. C., Ragozzine, D., et al. 2011, Science, 331, 562
- Cochran, W. D., Fabrycky, D. C., Torres, G., et al. 2011, ApJS, 197, 7
- Désert, J.-M., Charbonneau, D., Demory, B.-O., et al. 2011, ApJS, 197, 14
- Fabrycky, D. C., et al. 2012, accepted to ApJ
- Ford, E. B., Rowe, J. F., Fabrycky, D. C., et al. 2011, ApJS, 197, 2
- Ford, E. B., et al. 2012a, accepted to ApJ
- Holman, M. J., & Murray, N. W. 2005, Science, 307, 1288.
- Holman, M. J., Fabrycky, D. C., Ragozzine, D., et al. 2010, Science, 330, 51
- Lissauer, J. J., Fabrycky, D. C., Ford, E. B., et al. 2011a, Nature, 470, 53
- Lissauer, J. J., Ragozzine, D., Fabrycky, D. C., et al. 2011b, ApJS, 197, 8
- Rowe, J. F., et al. 2012, to be submitted to ApJS
- Slawson, R. W., Prša, A., Welsh, W. F., et al. 2011, AJ, 142, 160
- Steffen, J. H., Quinn, S. N., Borucki, W. J., et al. 2011, MNRAS, 417, L31
- Steffen, J. H., et al. 2012a, accepted to MNRAS
- Steffen, J. H., et al. 2012b, submitted to ApJ
- Tingley, B., Palle, E., Parviainen, H., et al. 2011, A&A, 536, L9
- Tremaine, S., & Dong, S. 2011, arXiv:1106.5403
- Veras, D., Ford, E. B., & Payne, M. J. 2011, ApJ, 727, 74
- Veras, D., & Ford, E. B. 2011, MNRAS, L369

Table 1. Kepler TTV Metrics Catalog Format

Column	Format	Description
1	KOI	F7.2 Kepler Object of Interest Identifier
2	S/N	F7.1 Photometric signal-to-noise for typical transit
3	nTT	I5 Number of transits used for analysis
4	T_{dur}	F5.1 Estimated transit duration (Batalha et al. 2012)
5	N_d	I2 Degree of polynomial selected for ephemeris
6	TTV Flag	I4 TTV Flag ^a
7	E_{lin}	F12.6 Epoch of best-fit linear ephemeris
8	$\sigma_{E_{lin}}$	F9.6 Uncertainty in E_{lin}
9	P_{lin}	F11.6 Period of best-fit linear ephemeris
10	$\sigma_{P_{lin}}$	F9.6 Uncertainty in P_{lin}
11	E_{N_d}	F12.6 Epoch of best-fit N_d -degree polynomial ephemeris
12	$\sigma_{E_{N_d}}$	F9.6 Uncertainty in E_{N_d}
13	P_{N_d}	F11.6 Period of best-fit N_d -degree polynomial ephemeris
14	$\sigma_{P_{N_d}}$	F9.6 Uncertainty in P_{N_d}
15	c_2	1X,G11.4 Coefficient of $P_{N_d} \times n^2$ for best-fit N_d -degree polynomial ephemeris ^b
16	σ_{c_2}	1X,G11.4 Uncertainty in c_2 ^b
17	c_3	1X,G11.4 Coefficient of $P_{N_d} \times n^3$ for best-fit N_d -degree polynomial ephemeris ^c
18	σ_{c_3}	1X,G11.4 Uncertainty in c_3 ^c
19	c_4	1X,G11.4 Coefficient of $P_{N_d} \times n^4$ for best-fit N_d -degree polynomial ephemeris ^d
20	σ_{c_4}	1X,G11.4 Uncertainty in c_4 ^d
21	σ_{TT}	F5.1 Median transit time uncertainty in minutes
22	MAD	F5.1 Median absolute deviation of transit times from a linear ephemeris in minutes
23	WRMS	F5.1 Weighted root mean square deviation of transit times from a linear ephemeris in minutes
24	$p_{\chi^2,lin}$	1X,G10.4 p -value for a χ^2 -test relative to linear ephemeris
25	$p_{\chi'^2,lin}$	1X,G10.4 p -value for a χ'^2 -test using χ'^2 relative to linear ephemeris ^e
26	$p_{\chi^2,quad}$	1X,G10.4 p -value for a χ^2 -test relative to quadratic ephemeris
27	$p_{\chi'^2,quad}$	1X,G10.4 p -value for a χ'^2 -test using χ'^2 relative to quadratic ephemeris ^e
28	$p_{\chi^2,cube}$	1X,G10.4 p -value for a χ^2 -test relative to cubic ephemeris
29	$p_{\chi'^2,cube}$	1X,G10.4 p -value for a χ'^2 -test using χ'^2 relative to cubic ephemeris ^e
30	$p_{\chi^2,quar}$	1X,G10.4 p -value for a χ^2 -test relative to quartic ephemeris
31	$p_{\chi'^2,quar}$	1X,G10.4 p -value for a χ'^2 -test using χ'^2 relative to quartic ephemeris ^e
32	$p_{F,quad,lin}$	1X,G10.4 p -value for an F -test comparing linear and quadratic ephemerides ^f
33	$p_{F,cube,lin}$	1X,G10.4 p -value for an F -test comparing linear and cubic ephemerides ^f
34	$p_{F,cube,quad}$	1X,G10.4 p -value for an F -test comparing quadratic and cubic ephemerides ^f
35	$p_{F,quar,lin}$	1X,G10.4 p -value for an F -test comparing linear and quartic ephemerides ^f
36	$p_{F,quar,quad}$	1X,G10.4 p -value for an F -test comparing quadratic and quartic ephemerides ^f
37	$p_{F,quar,cube}$	1X,G10.4 p -value for an F -test comparing cubic and quartic ephemerides ^f

^aSum of following flags: 1 if $p_{\chi^2} < 10^{-3}$, 2 if $p_{\chi'^2} < 10^{-3}$, 4 if $MAD \geq 5\sigma_{TT}$, 8 if $p_{F,lin,quad} < 0.02$ AND $nTT \geq 4$, 16 if $p_{F,lin,cube} < 0.02$ AND $nTT \geq 5$ AND IF(8-bit flag is set, $p_{F,quad,cube} < 0.02$, TRUE), and 32 if $p_{F,lin,quar} < 0.02$ AND $nTT \geq 8$ AND IF(16-bit flag is set, $p_{F,cube,quar} < 0.02$, IF(8-bit flag is set, $p_{F,quad,quar} < 0.02$, TRUE)).

^bZero if $N_d < 2$

^cZero if $N_d < 3$

^dZero if $N_d < 4$

^eFor description of χ'^2 statistic and tests, see § 3.1 of Ford et al. 2011

^fValue of -1.0 if insufficient number of transits

Note. — All ephemerides and TTV statistics are calculated from *Kepler* observations up to and including quarter six (Rowe et al. 2012).

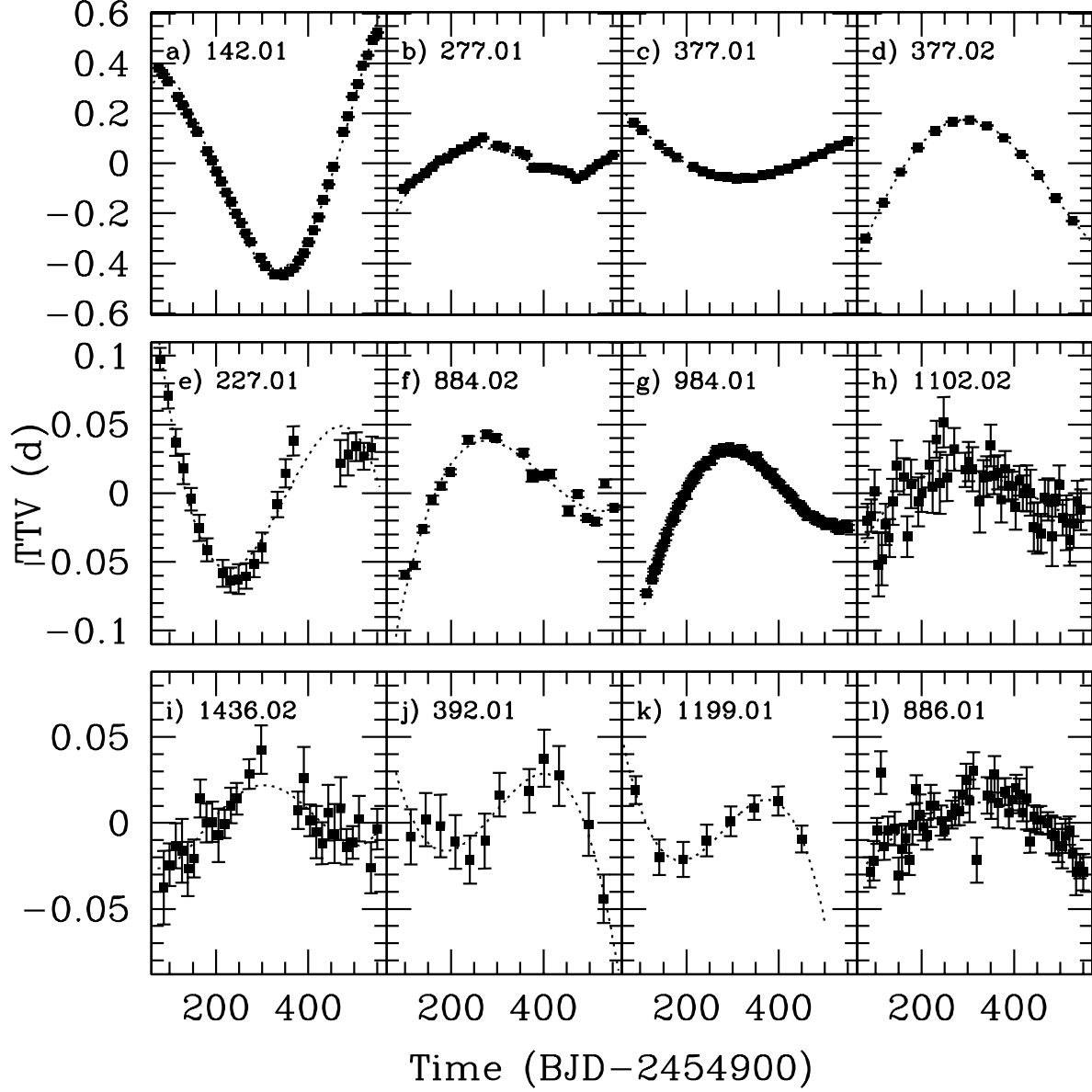


Fig. 1.— Transit times for planet candidates with long-term TTV trends. Dotted lines show the best-fit polynomial model given in Table 1. Kepler-9b (panel c) and Kepler-9c (panel d) have already been confirmed via TTVs (Holman et al. 2010). Similar figures for additional planet candidates will be available at <http://www.astro.ufl.edu/~eford/data/kepler/>.

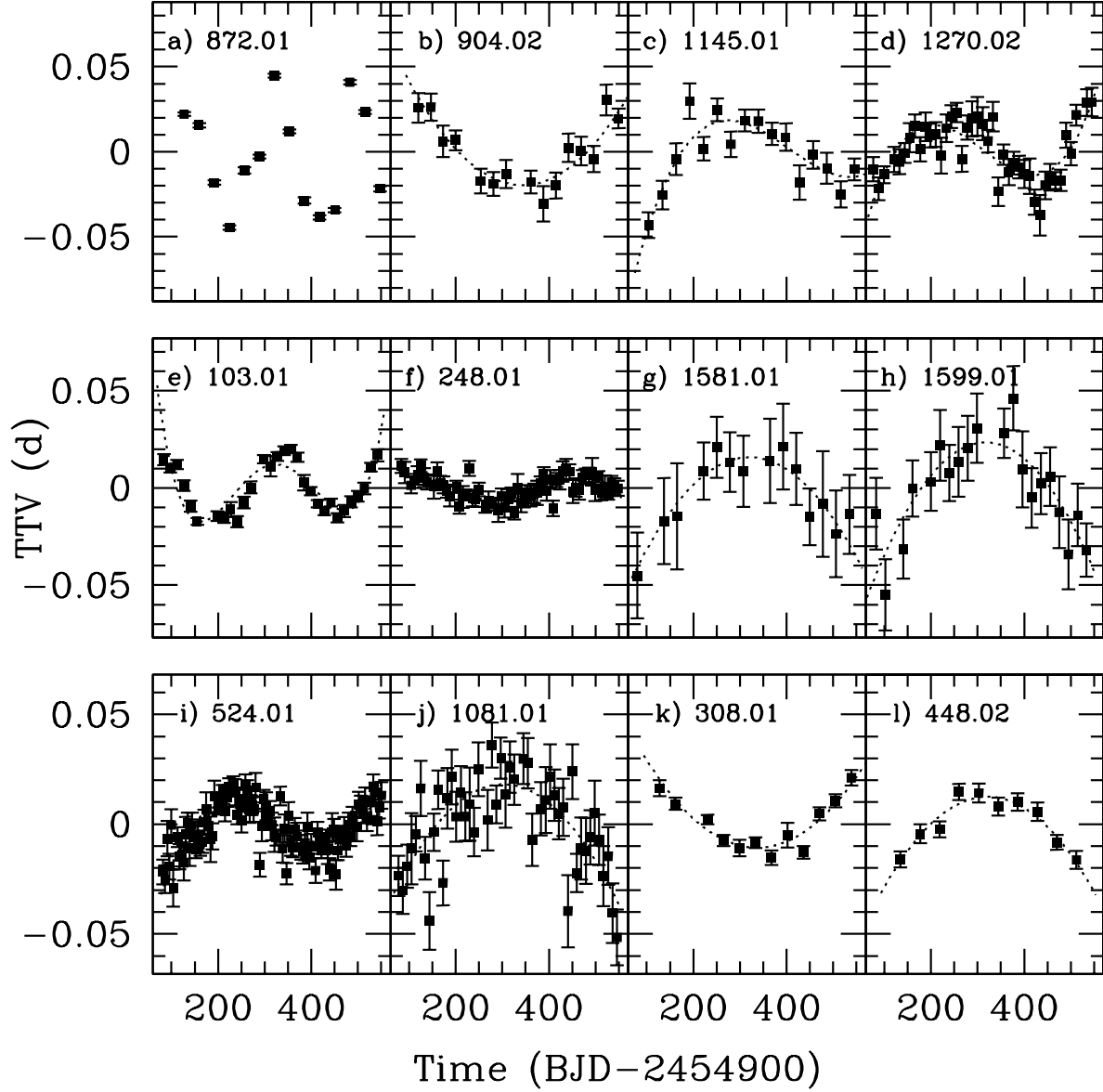


Fig. 2.— Transit times for planet candidates with long-term TTV trends. Dotted lines show the best-fit polynomial model given in Table 1. For KOI 872.01 (panel a) there is no polynomial model, since a polynomial model (of degree 4 or less) did not significantly improve upon the linear ephemeris.

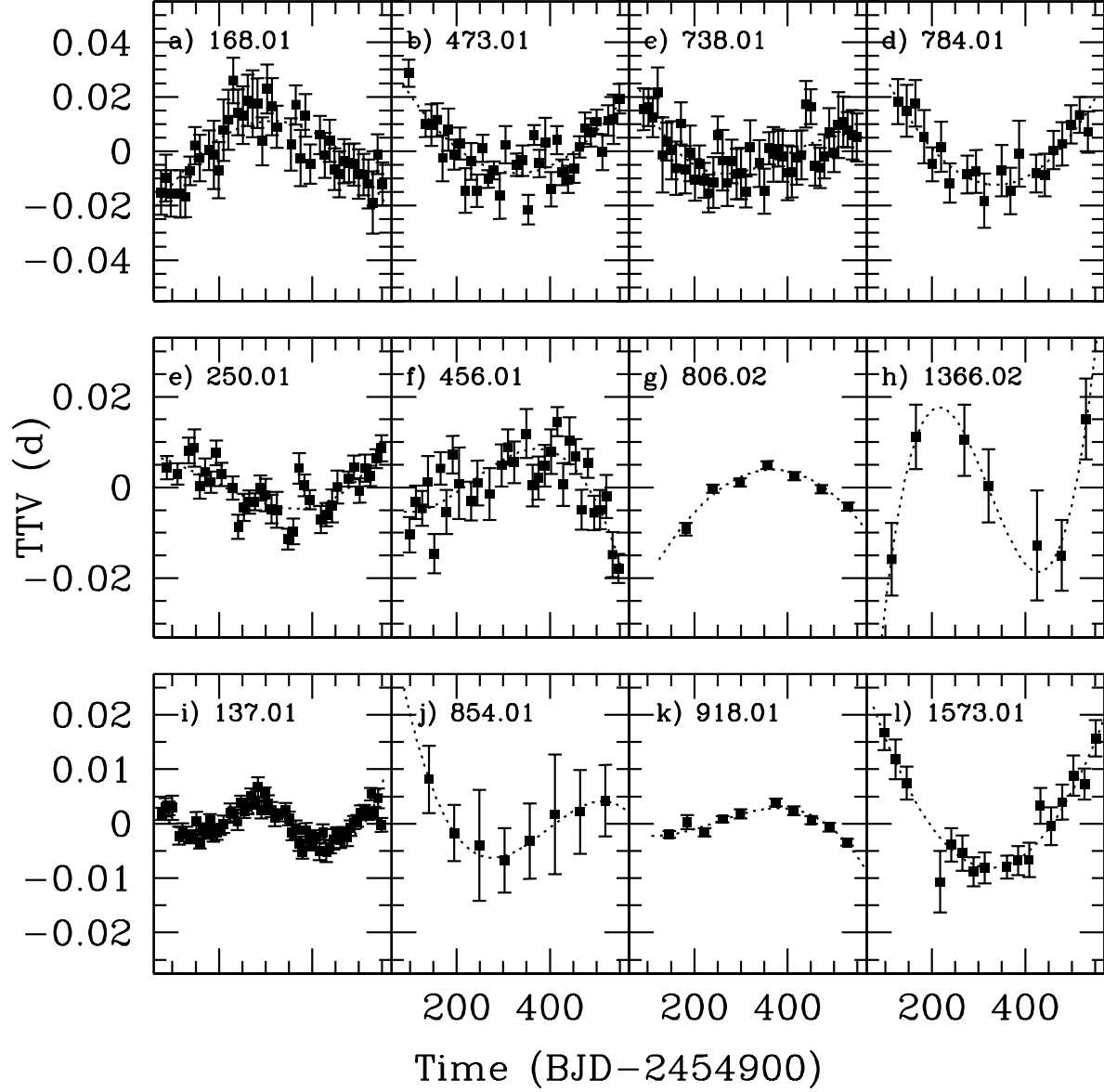


Fig. 3.— Transit times for planet candidates with long-term TTV trends. Dotted lines show the best-fit polynomial model given in Table 1. Kepler-18c (panel i) has already been confirmed via TTVs (Cochran et al. 2011).